Molecular alignment in a liquid induced by a nonresonant laser field: Molecular dynamics simulation

著者	藤村　勇一
journal or publication title	Journal of Chemical Physics
volume	120
number	19
page range	9123-9132
year	2004
URL	http://hdl.handle.net/10097/46256

doi: 10.1063/1.1704631

Molecular alignment in a liquid induced by a nonresonant laser field: Molecular dynamics simulation

Jun Ohkubo, Tsuyoshi Kato, Hirohiko Kono,[a] and Yuichi Fujimura
Department of Chemistry, Graduate School of Science, Tohoku University, Sendai 980-8578, Japan

(Received 11 November 2003; accepted 20 February 2004)

We carried out molecular dynamics (MD) simulations for a dilute aqueous solution of pyrimidine in order to investigate the mechanisms of field-induced molecular alignment in a liquid phase. An anisotopically polarizable molecule can be aligned in a liquid phase by the interaction with a nonresonant intense laser field. We derived the effective forces induced by a nonresonant field on the basis of the concept of the average of the total potential over one optical cycle. The results of MD simulations show that a pyrimidine molecule is aligned in an aqueous solution by a linearly polarized field of light intensity $I \sim 10^{13}$ W/cm^2 and wavelength $\lambda = 800$ nm. The temporal behavior of field-induced alignment is adequately reproduced by the solution of the Fokker–Planck equation for a model system in which environmental fluctuations are represented by Gaussian white noise. From this analysis, we have revealed that the time required for alignment in a liquid phase is in the order of the reciprocals of rotational diffusion coefficients of a solute molecule. The degree of alignment is determined by the anisotropy of the polarizability of a molecule, light intensity, and temperature. We also discuss differences between the mechanisms of optical alignment in a gas phase and a liquid phase. [DOI: 10.1063/1.1704631]

I. INTRODUCTION

Controlling the degrees of freedom of atoms and molecules is one of the main subjects of modern physics and chemistry. Laser light is now routinely used to cool, manipulate, and trap atoms.[1] The recent development of ultrashort, intense lasers has also provided new possibilities for controlling materials. It is known that intense laser fields induce exotic photochemical reactions or structural deformations of molecules such as bond stretching and bending.[2,3] Attempts have recently been made to control unimolecular reactions by optically tailored, intense-field laser pulses (of light intensity of $\sim 10^{14}$ W/cm^2).[4,5]

A molecule has an additional degree of freedom to control, namely, the spatial orientation of a molecule. Controlling the spatial alignment or orientation of molecules is recognized as an important manipulation in studies on chemical reaction and its control. There are several methods for controlling the alignment or orientation of molecules. Complete alignment means that molecules are arranged parallel to each other or parallel (or perpendicular) to the polarization direction of an applied field, and complete orientation means that molecules are all headed in a particular direction. A technique using a strong dc electric field has been applied to the control of the orientation of polar molecules, i.e., arranging polar molecules in a ''head vs tail'' orientation.[6,7] However, the static field technique cannot be use for aligning a nonpolar molecule because the anisotropic polarization energy of a nonpolar molecule induced by even a strong static field ($\sim 10^8$ V/m) does not create a sufficiently deep potential well to cause hindered molecular rotation. (Obviously, a static field cannot orient nonpolar molecules.)

To extend the control of alignment to a much broader class of molecules, Friedrich and Herschbach have proposed using a linearly polarized laser field to align nonpolar molecules.[8] If the polarizability of a molecule is anisotropic and the applied laser field is nonresonant with any electronic and vibrational transitions, the interaction of the laser electric field with the induced dipole moment of the molecule can render a deep anisotropic potential well leading to molecular alignment. Their proposal indicates an important new direction in molecular science because many techniques for laser-induced manipulation of molecules such as spatial trapping[8–10] and focusing,[11] in addition to alignment, were invented by the use of a strong nonresonant laser field.

The first verification of laser-induced alignment was given by Kim and Felker[12,13] in Raman spectroscopic studies of naphthalene trimers exposed to moderately strong laser fields (of light intensity of $I \sim 10^{10}$ W/cm^2). To align neutral molecules to a great extent, strong nonresonant nanosecond Nd:YAG laser pulses ($I \sim 10^{12}$ W/cm^2 and $\lambda \sim 1064$ nm) are used.[14] The corresponding electric field strength for this light intensity is as large as 2.7×10^9 V/m. The general applicability of the scheme has been demonstrated for I_2, ICl, CS_2, CH_3I, and C_6H_5I molecules. The strongest degree of alignment observed for I_2 is $\langle \cos^2 \theta \rangle = 0.81$, where θ is the angle between the field polarization direction and molecular axis. Transient alignment of molecules has also been achieved by using intense femtosecond pulses.[15] Recent experiments carried out by Larsen *et al.*[16] have demonstrated that an intense, elliptically polarized, nonresonant laser field can align planar molecules with the plane fixed in space, a finding that provides additional possibilities for controlling molecules. Villeneuve *et al.* have also performed an interesting experiment in which the bond of Cl_2 is broken by rotating the direction

[a]Electronic mail: kono@mcl.chem.tohoku.ac.jp

of the field polarization, i.e., by the centrifugal force generated.[17]

All of the experiments described above have been carried out in gas phases, and the mechanisms have been clarified.[8] On the other hand, most of the interesting photoinduced reactions are conducted in liquid phases. When irradiated by linearly polarized light, cigarlike-shaped photochromic molecules undergo photoisomerization cycles (e.g., $trans \rightarrow cis \rightarrow trans$ photoisomerization of azo derivatives) and tend to line up in a direction perpendicular to the polarization direction of the excitation (Weigert effect).[18] This photoinduced anisotropy (PIA) has been observed in viscous liquids and polymers containing an azo derivative.[19] Three different processes participate in PIA: angular hole burning (AHB), angular redistribution (AR), and rotational diffusion (RD).[20]

In PIA, the molecules excited with polarized light align in a direction perpendicular to the polarization, but the dipole moments of the molecules are not oriented to one direction (i.e., they are centrosymmetric). Creation of noncentrosymmetry can be induced in a polymer, even below its glass transition temperature, by photoassisted poling (PAP), i.e., by the application of a dc electric field in addition to a pumping optical pulse.[21] The random and isotropic feature of angular redistribution in PIA is broken by the torque exerted by the dc field on the molecules. Another way to induce noncentrosymmetry is all-optical poling (AOP).[22] A coherent superposition with the appropriate phase difference of two optical waves, one at frequency ω and another at 2ω, yields a noncentrosymmetric resultant field by combination of the two electric fields E_{ω} and $E_{2\omega}$. It has also been reported that this poling method is applicable to molecules that absorb neither ω nor 2ω.[23]

To describe the fundamental mechanisms of PIA and PAP, Dumont has incorporated the effects of AHB and AR into the rotational diffusion equation for a dye molecule.[24] Although it is very laborious to go beyond this kind of phenomenological effective model for PIA and PAP, microscopic dynamics of molecules in liquids interacting with laser fields must be investigated. In this study, as the first step, the alignment dynamics of a solute molecule (and solvent molecules) in an aqueous solution interacting with a nonresonant laser field was investigated by molecular dynamics (MD) simulation. In contrast to alignment in a gas phase, little is known about liquid-phase molecular dynamics in a nonresonant laser field. Results of studies on the dynamics of field-induced alignment in a liquid phase will be very useful for establishing methods to control of chemical reactions or photophysical processes in a liquid phase.[25]

MD simulations describing the effects of an externally applied electric field on a molecular liquid were initiated by Evans in a series of publications.[26–29] Taking into account the permanent molecular dipole moment (an unpolarizable molecular model), he discussed the dispersion of the induced orientation anisotropy in a liquid sample caused by a CO_2 laser field.[28] MD simulation has also been used to study the time-dependent response of ionic liquids to an alternating field (wavelength $\lambda < 1$ mm).[30,31] In the study of electrical conductivity of an electrolyte, it is sufficient to consider only the interaction between the applied electric field and the formal charges of ions in the molten salt as the main interaction with the field.

In order to discuss molecular alignment in a liquid, it is definitely necessary to employ polarizable models. Since the anisotropic polarization energy of a molecule exerts torque on the molecule, it is essential to deal with the anisotropy of molecular polarizability as precisely as possible. There are some methods for calculating the polarization energy in a MD simulation. The most frequently used method is based on decomposition of molecular polarizabilities into atomic polarizabilities or construction of molecular polarizabilities from (model) isotropic atomic polarizabilities.[32–34] Although most of the methods assign different values of the atomic polarizability to atoms that have different molecular environments,[35] the effective atomic polarizabilities were uniquely determined.[36] The polarizabilities of groups or sites in a molecule can be constructed from the effective atomic polarizabilities. This approach using atomic polarizabilities is relatively easy to implement in MD simulation,[34] but caution must be exercised as to how well the methods describe polarizabilities in the condensed phase where distances between highly polar and/or ionic groups are on the order of bonding distances.[37]

Fluctuating charge models have also been employed to take account of polarization effects. In the fluctuating charge models,[38,39] the (atomic) sites of point charges are fixed in a molecular frame but the charges are instantaneously varied in magnitude according to the strength and direction of the total electric field on the charge site. The adjustable parameters involved are determined so that the degree of molecular polarizability in the condensed phase is reflected. Robinson *et al.* have investigated effects of an intense laser field on liquid water by using MD simulations and a SPC-FP water model, which is constructed by introducing a fluctuating charge model in the simple point charge (SPC) water model.[40] They have reported that under the influence of the strong external torque, both the liquid structure and the intramolecular geometry are distorted.

Berne *et al.* have also developed a fluctuating charge model in which the point charges on atomic sites are allowed to vary in response to the environment so that electronegativity equalization is satisfied, and applied it to water using the simple point charge (SPC) and the four-point transferable intermolecular potential (TIP4P).[41,42] Using the new fluctuating charge (FQ) force models, English and MacElroy performed molecular dynamics simulations of water in the presence of external electromagnetic fields to investigate molecular mobility and hydrogen bonding patterns in the microwave to far-infrared frequency range.[43] The electric field strength applied ranges from $\sim 5 \times 10^8$ V/m to $\sim 3 \times 10^9$ V/m (up to light intensity of $I \sim 10^{12}$ W/cm^2). Although the results indicate the potential ability of fluctuating charge force models, the range of application is limited. The polarizable force field based on the FQ model has been so far developed mainly for water,[41,42] although Berne *et al.* have presented a general procedure to construct a FQ model that reproduces both the intramolecular energetics and the many-body polarization response of *ab initio* quantum mechanics

and parametrized a polarizable force field for polyalanine from the FQ model.[44]

MD simulation has also been used to study orientational and collision-induced light scattering (LS) in liquids. In the MD study of LS, the molecular polarizability is used to evaluate the collective polarizability of which the relaxation describes LS spectra. The intermolecular dipole-induced dipole (DID) interactions are evaluated as interactions between molecular centers (the center–center DID model); that is, the polarizability is treated as concentrated in the center of mass of the molecule. This method of evaluation is expected to be valid in the case of small molecules or in the case where an intense uniform electric field is applied to a liquid sample. In most of the MD studies of LS,[45–47] the collective polarizability is approximated by an expression based on first-order perturbation theory (which is a second-order expression with respect to molecular polarizabilities).[48] The relative importance of higher-order DID interactions has been investigated by Ladani *et al.*[49–52] The MD simulations have shown that at liquid densities, effects of higher-order DID interaction are very important for highly polarizable fluids such as CS_2, but much less significant for relatively weakly polarizable ones such as O_2 and N_2. In the calculation of the collective polarizability, the trajectories are solely determined by the atom–atom Lennard-Jones potentials (+ Coulomb potentials) and the forces originating from the induced dipoles are not included. The advantage of using molecular polarizabilities is that molecular polarizabilities can be calculated by *ab initio* molecular orbital methods and the values experimentally determined in the gas phase are mostly available.

Our mission here is not to develop the ultimate method for molecular dynamics in a liquid interacting with intense laser fields, but rather to assess, in a computationally tractable way, the degree of field-induced molecular alignment in a liquid. Therefore, to investigate optical alignment in a liquid phase, in this study, we adopt a simple model in which the molecular polarizabilities are placed at the center of mass of the molecule as in the center–center DID interaction model.

The structure of this paper is as follows: In Sec. II, a MD method for calculating the effects of interactions between molecules and nonresonant laser fields is presented. We calculate the field-induced forces for molecular rotation, and explain the mechanism of optical alignment. The results of MD simulations for a pyrimidine aqueous solution interacting with a nonresonant intense laser field ($\lambda = 800$ nm) are given in Sec. III. The results of analysis based on the Fokker–Planck equation are also presented to clarify the mechanism of optical alignment of pyrimidine in an aqueous solution.

II. THEORY

A. Effects of an external laser field

To investigate the alignment dynamics of molecules interacting with a nonresonant intense laser field in a liquid phase, we consider polarization energies as well as the Lennard-Jones and Coulomb interactions. In the case of interaction with a nonresonant laser field, the spatial homogeneity of the applied field is much larger than the sizes of molecules. The polarization induced by a uniform laser electric field (field-induced dipole moment) can be reproduced by using molecular polarizabilities. In the following, outlining the general framework of the theoretical treatment, we describe the procedure for calculating the dominant torque caused by the interaction between a nonresonant laser field and the anisotropic polarization of a molecule.

To discuss alignment dynamics, it is sufficient to treat a molecule as a rigid body. Therefore, we fix the structures of molecules. Then, the Lennard-Jones potential energy U_{LJ} and the Coulomb potential energy U_{Coulomb} of a system are given by

$$U_{\mathrm{LJ}} = \sum_{k>l} 4\epsilon_{kl} \left\{ \left(\frac{\sigma_{kl}}{r_{kl}^{\mathrm{atom}}} \right)^{12} - \left(\frac{\sigma_{kl}}{r_{kl}^{\mathrm{atom}}} \right)^{6} \right\}, \tag{1}$$

and

$$U_{\mathrm{Coulomb}} = \sum_{k>l} \frac{1}{4\pi\varepsilon_0} \frac{q_k q_l}{r_{kl}^{\mathrm{atom}}}. \tag{2}$$

where r_{kl}^{atom} is the distance between atom l and atom k, q_k and q_l are atomic charges, ϵ_0 is the vacuum permittivity, and ϵ_{kl} and σ_{kl} are constants for the potential depth and range. Only atoms k and l that belong to different molecules are counted in Eqs. (1) and (2).

As mentioned above, the polarization energies caused by a laser field must be added to the sum of Eqs. (1) and (2). We here examine polarization effects due to a nonresonant laser field. The total polarization energy $U_{\mathrm{pol}}^{\mathrm{add}}(t)$ in the dipole approximation can be expressed by quantities assigned to molecules,[32]

$$U_{\mathrm{pol}}^{\mathrm{add}}(t) = -\frac{1}{2} \sum_i \boldsymbol{\mu}_i \cdot (\mathbf{E}_{\mathrm{ext}}(t) + \mathbf{E}_i^o), \tag{3}$$

where $\mathbf{E}_{\mathrm{ext}}(t)$ is the applied laser electric field at time t, $\mathbf{E}_i^o$ is the local electric field on the ith molecule due to the permanent charges of other molecules, and $\boldsymbol{\mu}_i$ is the total induced dipole moment vector of molecule i. (Note that the indexes i belong to molecules, not to atoms.) Here, we define a dipole field tensor $\mathbf{T}_{ij}$ expressed as

$$\mathbf{T}_{ij} = \frac{1}{4\pi\varepsilon_0} \left(\frac{3\mathbf{r}_{ij}\mathbf{r}_{ij}}{r_{ij}^5} - \frac{1}{r_{ij}^3}\mathbf{I} \right), \tag{4}$$

with

$$\mathbf{r}_{ij}\mathbf{r}_{ij} = \begin{pmatrix} X_{ij}^2 & X_{ij}X_{ij} & X_{ij}Z_{ij} \\ X_{ij}Y_{ij} & Y_{ij}^2 & Y_{ij}Z_{ij} \\ X_{ij}Z_{ij} & Y_{ij}Z_{ij} & Z_{ij}^2 \end{pmatrix}, \tag{5}$$

where $\mathbf{r}_{ij}$ is the vector from the center of mass of molecule j to that of molecule i, $\mathbf{I}$ is the identity matrix, and X_{ij}, Y_{ij}, and Z_{ij} are the Cartesian components of $\mathbf{r}_{ij}$. Using the dipole field tensor $\mathbf{T}_{ij}$, we can write $\boldsymbol{\mu}_i$ as

$$\boldsymbol{\mu}_i = \boldsymbol{\alpha}_i \left(\mathbf{E}_{\mathrm{ext}}(t) + \mathbf{E}_i^o + \sum_{j \neq i} \mathbf{T}_{ij}\boldsymbol{\mu}_j \right), \tag{6}$$

where $\boldsymbol{\alpha}_i$ is the polarizability tensor of molecule i. Here, we refer to the first term $\boldsymbol{\alpha}_i \mathbf{E}_{\mathrm{ext}}(t)$ as the field-induced dipole

moment and refer to the second term $\boldsymbol{\alpha}_i \mathbf{E}_i^o$ as the charge-induced dipole moment. The electric fields and the quantities $\boldsymbol{\alpha}_i$ and $\boldsymbol{\mu}_i$ are defined in a space-fixed coordinate system.

As we discussed later, in an intense laser field, the dipole field $\Sigma_{j\neq i}\mathbf{T}_{ij}\boldsymbol{\mu}_j$ is much smaller than $\mathbf{E}_{\mathrm{ext}}(t)+\mathbf{E}_i^o$. Therefore, resorting to perturbation theory as in Refs. 45–47, we approximate Eq. (6) as

$$\boldsymbol{\mu}_i \simeq \boldsymbol{\alpha}_i \left\{ \mathbf{E}_{\mathrm{ext}}(t)+\mathbf{E}_i^o+\sum_{j\neq i} \mathbf{T}_{ij}\boldsymbol{\alpha}_j\left(\mathbf{E}_{\mathrm{ext}}(t)+\mathbf{E}_j^o\right)\right\}. \tag{7}$$

We thus can express Eq. (3) as

$$\begin{aligned}\mathbf{U}_{\mathrm{pol}}^{\mathrm{add}} &\simeq U_{\mathrm{pol}}(t)\\ &= -\frac{1}{2}\sum_i \boldsymbol{\alpha}_i\left\{ \mathbf{E}_{\mathrm{ext}}(t)+\mathbf{E}_i^o+\sum_{j\neq i} \mathbf{T}_{ij}\boldsymbol{\alpha}_j(\mathbf{E}_{\mathrm{ext}}(t)\right.\\ &\quad \left.+\mathbf{E}_j^o)\right\}\cdot(\mathbf{E}_{\mathrm{ext}}(t)+\mathbf{E}_i^o).\end{aligned} \tag{8}$$

Since the period of a nonresonant laser field of ~800 nm, $2\pi/\omega_L$, where ω_L is the field frequency, is $\lesssim$3 fs, the molecules can be assumed to freeze over an optical cycle. Then, we can replace $U_{\mathrm{pol}}(t)$ by the average of $U_{\mathrm{pol}}(t)$ over one optical cycle (cycle average),

$$\begin{aligned}\langle U_{\mathrm{pol}}(t)\rangle_{\mathrm{cycle}} &= -\frac{1}{2}\sum_i \langle \mathbf{E}_{\mathrm{ext}}(t)\cdot\boldsymbol{\alpha}_i\cdot\mathbf{E}_{\mathrm{ext}}(t)\rangle_{\mathrm{cycle}}\\ &\quad -\frac{1}{2}\sum_i \left\langle\left(\sum_{j\neq i}\mathbf{T}_{ij}\boldsymbol{\alpha}_j\mathbf{E}_{\mathrm{ext}}(t)\right)\cdot\boldsymbol{\alpha}_i\cdot\mathbf{E}_{\mathrm{ext}}(t)\right\rangle_{\mathrm{cycle}}\\ &\quad -\frac{1}{2}\sum_i \mathbf{E}_i^o\cdot\boldsymbol{\alpha}_i\cdot\mathbf{E}_i^o\\ &\quad -\frac{1}{2}\sum_i \left(\sum_{j\neq i}\mathbf{T}_{ij}\boldsymbol{\alpha}_j\mathbf{E}_j^o\right)\cdot\boldsymbol{\alpha}_i\cdot\mathbf{E}_i^o,\end{aligned} \tag{9}$$

where $\langle A(t)\rangle_{\mathrm{cycle}} \equiv \int_{t-\pi/\omega_L}^{t+\pi/\omega_L} A(t')dt'$. We have used the condition that the nuclei of molecules do not move during an optical cycle. Then, the correlation between $\mathbf{E}_i^o$ and $\mathbf{E}_{\mathrm{ext}}(t)$ do not exist, for instance,

$$\langle \mathbf{E}_i^o\cdot\boldsymbol{\alpha}_i\cdot\mathbf{E}_{\mathrm{ext}}(t)\rangle_{\mathrm{cycle}} = \mathbf{E}_i^o\cdot\boldsymbol{\alpha}_i\cdot\langle\mathbf{E}_{\mathrm{ext}}(t)\rangle_{\mathrm{cycle}} = 0. \tag{10}$$

The last term in Eq. (9) corresponds to the first-order correction in the calculation of collective polarizability.[45–47] The last two terms in Eq. (9) originating from the interaction associated with the electric field due to the permanent charges and the resultant charge-induced dipoles exist even in the absence of an external field $\mathbf{E}_{\mathrm{ext}}(t)$. We assume that the effects of interactions of this type are already included in the molecular models adopted in our MD simulations. Considering the fact that the value of the permanent dipole of the TIP4P water model we employ, 2.18 D, is larger than the experimentally observed value in a molecular beam of water (1.85 D), this assumption is reasonable. Therefore, using the first term in Eq. (9), we define the effective polarization energy of the zeroth-order approximation, $U_{\mathrm{pol}}^{\mathrm{eff,0th}}(t)$, as below,

$$\begin{aligned}U_{\mathrm{pol}}^{\mathrm{eff,0th}}(t) &= -\frac{1}{2}\sum_i \mathbf{E}_{\mathrm{ext}}(t)\cdot\boldsymbol{\alpha}_i\cdot\mathbf{E}_{\mathrm{ext}}(t)\\ &= -\frac{1}{2}\sum_i \boldsymbol{\mu}_{i,\mathrm{ext}}\cdot\mathbf{E}_{\mathrm{ext}}(t),\end{aligned} \tag{11}$$

where $\boldsymbol{\mu}_{i,\mathrm{ext}}$ is the field-induced dipole moment of the ith molecule, i.e., $\boldsymbol{\alpha}_i\cdot\mathbf{E}_{\mathrm{ext}}(t)$. Similarly, we define the polarization of the first-order approximation for the sum of the first two terms in Eq. (9),

$$U_{\mathrm{pol}}^{\mathrm{eff,1st}}(t) = -\frac{1}{2}\sum_i \boldsymbol{\mu}_{i,\mathrm{ext}}\cdot\left(\mathbf{E}_{\mathrm{ext}}(t)+\sum_{j\neq i}\mathbf{T}_{ij}\boldsymbol{\alpha}_j\mathbf{E}_{\mathrm{ext}}(t)\right). \tag{12}$$

Thus, the total potential energy of the system can be expressed by the sum of the three terms

$$U_{\mathrm{total}} = U_{\mathrm{LJ}}+U_{\mathrm{Coulomb}}+U_{\mathrm{pol}}^{\mathrm{eff}}, \tag{13}$$

where $U_{\mathrm{pol}}^{\mathrm{eff}}$ is either $U_{\mathrm{pol}}^{\mathrm{eff,0th}}(t)$ or $U_{\mathrm{pol}}^{\mathrm{eff,1st}}(t)$. In Sec. III, we will discuss the difference between these two effective polarization energies.

We next derive a formula to calculate the forces due to the effective polarization energy of Eq. (12) in a rigid body model. Because the laser field is spatially uniform, it generates no translational forces on molecules through polarization energy. Therefore, we consider only the rotational forces (torque) here. A transformation between a space-fixed coordinate system and a body-fixed coordinate system can be expressed as[53]

$$\boldsymbol{\mu}_{i,\mathrm{ext}} = \mathbf{A}_i^T\tilde{\boldsymbol{\mu}}_{i,\mathrm{ext}} \tag{14}$$

where $\mathbf{A}_i$ is the orthogonal matrix for transformation, the superscript T denotes a transposed matrix, and $\tilde{\boldsymbol{\mu}}_{i,\mathrm{ext}}$ is the field-induced dipole moment in the body-fixed coordinate system. Using this expression, we can express the torque about a body-fixed x axis of the mth molecule as follows:

$$\begin{aligned}\mathbf{F}_{m,\mathrm{pol}}^{\Omega_x} &= \frac{\partial}{\partial\Omega_x}\left\{\frac{1}{2}\boldsymbol{\mu}_{m,\mathrm{ext}}\cdot\left(\mathbf{E}_{\mathrm{ext}}(t)+\sum_{j\neq m}\mathbf{T}_{mj}\boldsymbol{\alpha}_j\mathbf{E}_{\mathrm{ext}}(t)\right)\right\}\\ &= \frac{1}{2}\left\{\mathbf{E}_{\mathrm{ext}}^T(t)\frac{\partial\mathbf{A}_m^T}{\partial\Omega_x}\tilde{\boldsymbol{\alpha}}_m\mathbf{A}_m\right.\\ &\quad\times\left(\mathbf{E}_{\mathrm{ext}}(t)+\sum_{j\neq m}\mathbf{T}_{mj}\boldsymbol{\alpha}_j\mathbf{E}_{\mathrm{ext}}(t)\right)\\ &\quad+\mathbf{E}_{\mathrm{ext}}^T(t)\mathbf{A}_m^T\tilde{\boldsymbol{\alpha}}_m\frac{\partial\mathbf{A}_m}{\partial\Omega_x}\\ &\quad\left.\times\left(\mathbf{E}_{\mathrm{ext}}(t)+\sum_{j\neq m}\mathbf{T}_{mj}\boldsymbol{\alpha}_j\mathbf{E}_{\mathrm{ext}}(t)\right)\right\},\end{aligned} \tag{15}$$

where Ω_x is a rotation angle about the body-fixed x axis and $\tilde{\boldsymbol{\alpha}}_m$ is the polarizability tensor of the mth molecule in the body-fixed coordinate system. In the case of the zeroth-order approximation of Eq. (11), the torque is given by setting $\mathbf{T}_{mj}=\mathbf{0}$ in Eq. (15). The torques forces about other axes are described similarly. Thus, what is necessary for MD simulation in the presence of a nonresonant laser field is only to

incorporate the effective polarization energy of Eq. (11) [or Eq. (12)] and the torques of the form of Eq. (15) into the conventional MD algorithm.[53]

If the polarizability tensor $\tilde{\boldsymbol{\alpha}}_m$ is isotropic, we can express the polarizability as

$$\tilde{\boldsymbol{\alpha}}_m = \alpha_m^o \mathbf{I}, \tag{16}$$

where α_m^o is a scalar. Using this polarizability, the torque is expressed as

$$\mathbf{F}_{m,\mathrm{pol}}^{\Omega_x} = \frac{1}{2}\mathbf{E}_{\mathrm{ext}}^T(t)\,\alpha_m^o\left(\frac{\partial \mathbf{A}_m^T}{\partial \Omega_x}\mathbf{A}_m + \mathbf{A}_m^T\frac{\partial \mathbf{A}_m}{\partial \Omega_x}\right) \times\left(\mathbf{E}_{\mathrm{ext}}(t) + \sum_{j\neq m}\mathbf{T}_{mj}\boldsymbol{\alpha}_j\mathbf{E}_{\mathrm{ext}}(t)\right) = 0. \tag{17}$$

Here we have used

$$\frac{\partial \mathbf{A}_m^T}{\partial \Omega_x}\mathbf{A}_m + \mathbf{A}_m^T\frac{\partial \mathbf{A}_m}{\partial \Omega_x} = \mathbf{0}, \tag{18}$$

because the matrix $\mathbf{A}_m$ is orthogonal ($\mathbf{A}_m^T\mathbf{A}_m = \mathbf{I}$). In conclusion, an isotropic polarizability tensor causes no torque, as expected.

B. Mechanism of optical alignment

The interaction between a nonresonant, linearly polarized laser field and the field-induced dipole moment of a molecule creates a potential minimum with respect to the molecular orientation, forcing them to librate over a limited angular range along the polarization axis of the field instead of rotating freely with random spatial orientations. To explain the origin of alignment, in this subsection, we neglect the interactions between field-induced dipole moments. Then, the interaction energy between the applied laser field and a molecule is expressed as

$$V_{\mathrm{ext}}(t) = -\boldsymbol{\mu}_{\mathrm{per}}\cdot\mathbf{E}_{\mathrm{ext}}(t) - \tfrac{1}{2}\mathbf{E}_{\mathrm{ext}}(t)\cdot\boldsymbol{\alpha}\cdot\mathbf{E}_{\mathrm{ext}}(t), \tag{19}$$

where $\boldsymbol{\mu}_{\mathrm{per}}$ is the permanent dipole moment of the molecule.

We assume that the applied laser electric field $\mathbf{E}_{\mathrm{ext}}$ at time t takes the form

$$\mathbf{E}_{\mathrm{ext}}(t) = \hat{e}_Z E_0 \sin(\omega_L t), \tag{20}$$

where the polarization direction $\hat{e}_Z$ is the unit vector along the space-fixed Z axis, E_0 is the field strength, and ω_L is the field frequency. If the electric field is nonresonant with any electronic transitions and oscillates at optical frequencies ω_L (e.g., near-infrared light), $V_{\mathrm{ext}}(t)$ can be replaced by the time-averaged one over a short optical cycle: then, the interaction between the field and the permanent dipole moment, $-\boldsymbol{\mu}_{\mathrm{per}}\cdot\mathbf{E}_{\mathrm{ext}}(t)$, vanishes.[54] Since the cycle-average of $\{\mathbf{E}_{\mathrm{ext}}(t)\}^2$ is $E_0^2/2$,[54] only the interaction between the field and the polarization remains. We finally obtain the simple polarization energy of a molecule, U_{pol}^o, for the cycle-average of $V_{\mathrm{ext}}(t)$,

$$U_{\mathrm{pol}}^o = -\tfrac{1}{4}E_0^2(\alpha_{xx}\sin^2\psi\sin^2\theta + \alpha_{yy}\cos^2\psi\sin^2\theta + \alpha_{zz}\cos^2\theta), \tag{21}$$

where ψ and θ are Euler angles,[55] and the axes x, y, and z are chosen to be the principal axes of the polarizability tensor of the molecule (see, for instance, Fig. 1). Here, α_{xx}, α_{yy}, and α_{zz} are the polarizabilities in the body-fixed coordinate system. If there is no anisotropy in polarizabilities, U_{pol}^o is isotropic: no alignment occurs.

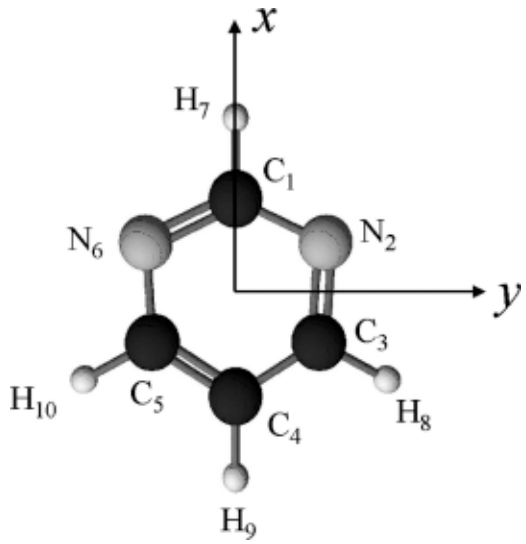

FIG. 1. Structure of a pyrimidine molecule and definitions of the molecular axes. The z axis is perpendicular to the $x-y$ plane.

To show an example for alignment, let us suppose a simple case in which the molecule is linear. In this simple case, $\alpha_{xx} = \alpha_{yy} = \alpha_\perp$, $\alpha_{zz} = \alpha_\parallel$ and $\psi = 0°$, and we obtain from Eq. (21),

$$U_{\mathrm{pol}}^{\mathrm{lincar}} = -\tfrac{1}{4}E_0^2\{(\alpha_\parallel - \alpha_\perp)\cos^2\theta + \alpha_\perp\}. \tag{22}$$

For a molecule with $\alpha_\parallel > \alpha_\perp$, this equation shows potential minima around $\theta = 0°$ and $\theta = 180°$. This will align the molecule parallel to the space-fixed polarization direction Z.

C. Details of the MD simulation

As a first step to demonstrate optical alignment in a liquid phase, we carried out MD simulations for a dilute aqueous solution of pyrimidine. A molecule that has large anisotropic polarizability is favorable for optical alignment. For example, large molecules such as dye molecules generally have large anisotropic polarizability. However, reliable MD parameters in the total potential energy are not available for such molecules. Moreover, it is time-consuming to run a MD simulation for sophisticatedly modeled large molecules and it is difficult to analyze the results. For these reasons, we selected an intermediate-sized molecule, a pyrimidine molecule, for which the MD parameters in a rigid body model have been determined.[56]

We carried out simulations of 255 TIP4P water molecules[57,58] and one pyrimidine molecule.[56] (One water molecule in an ensemble of 256 water molecules with a density of 1.00 g/cm^3 is replaced by a pyrimidine molecule.) The atomic charges and other parameters used in the simulations are summarized in Table I. The Lennard-Jones coefficients of pyrimidine are $\sigma_k = 3.11815$, 3.29632, and 2.74397 Å for nitrogen, carbon, and hydrogen, respectively, while $\epsilon_k = 0.16$, 0.12, and 0.01 kcal/mol, respectively. In addition, we used the combination rules for Eq. (1),

TABLE I. Values of atomic coordinates with respect to the center of mass of a pyrimidine molecule and the magnitudes of the associated point charges q in units of e. The molecule and axis system are sketched in Fig. 1.

Center	x (Å)	y (Å)	z (Å)	Charges q
C_1	1.2802	0	0	0.8613
N_2	0.6886	1.2023	0	−0.9006
C_3	−0.6513	1.1864	0	0.7944
C_4	−1.3812	0	0	−0.9997
C_5	−0.6513	−1.1864	0	0.7944
N_6	0.6886	−1.2023	0	−0.9006
H_7	2.3792	0	0	0.0197
H_8	−1.1548	2.1629	0	0.0208
H_9	−2.4802	0	0	0.2895
H_{10}	−1.1548	−2.1629	0	0.0208

$$\epsilon_{kl}=\sqrt{\epsilon_k\epsilon_l},\quad \sigma_{kl}=\frac{\sigma_k+\sigma_l}{2}. \tag{23}$$

The components of the molecular polarizability of a water molecule are $\alpha_{xx}=1.286\ \text{Å}^3$, $\alpha_{yy}=1.626\ \text{Å}^3$, and $\alpha_{zz}=1.495\ \text{Å}^3$,[59] where the x axis is along the dipole moment of a water molecule and the water molecule is in the $x-y$ plane. Those of a pyrimidine molecule are $\alpha_{xx}=8.58\ \text{Å}^3$, $\alpha_{yy}=10.10\ \text{Å}^3$, and $\alpha_{zz}=5.21\ \text{Å}^3$.[60]

The simulations were carried out in an *NVT* ensemble. The wavelength of the applied electric field in Eq. (20), $\lambda=2\pi c/\omega_L$, was assumed to be 800 nm of Ti:Sapphire laser, which is out of the absorption bands of pyrimidine and water molecules. In the case of the interaction with a 800 nm picosecond pulse ($I\sim10^{13}$ W/cm^2), the temperature of water does not increase. To reflect this fact, we used a Nosé–Hoover chain thermostat[53] to keep the temperature of water constant around its desired value (298 K). The Nosé–Hoover chain thermostat was set not to interact with the pyrimidine molecule so that the dynamics of the solute molecule is not directly influenced by the thermostat. The hierarchy of the Nosé–Hoover chain thermostat was threefold. In a Nosé–Hoover thermostat, the temperature of the system is feedback-controlled by coupling it to one additional degree of freedom, s, which acts like an external reservoir. The heat bath s is characterized by its masslike parameter Q which determines how quickly the system is thermostatted. The response of a thermostat is controlled by the relaxation time which is defined as $\tau^2=Q/2K_0$, where K_0 is the value of the kinetic energy corresponding to the required value of the temperature.[61] We set $\tau=50$ fs for the first thermostat. Parameters of the second and third thermostats were tuned similarly so that the temperature of water does not increase during the interaction of a 800 nm picosecond pulse.

The equations of motion for the rigid-body model were solved numerically using the Gear predictor–corrector algorithm with a time step of 0.2 fs.[53] Periodic boundary conditions were used. (The length of a side of the basic cube cell is about 19 Å.) A cutoff sphere of radius of 15 Å was used for evaluating the Lennard-Jones potential energy. The Coulomb potentials were calculated by using the Ewald method.[53] In addition, we neglected the interaction between the field and the permanent dipole moments (or charges), as justified in Sec. II. For calculation of the polarization energy of Eq. (11), we do not need potential cutoff because the zeroth-order approximation method considers only polarization interactions between an external electric field and each molecule. For the first-order approximation method of Eq. (12), we introduced a spherical cutoff of 15Å, as in the treatment of the first-order DID interactions.[45–47] Although straightforward spherical truncation of the long range dipole–dipole interactions may in general cause even qualitative errors, the estimation of Eq. (12) by the use of a spherical cutoff is justified in the presence of an intense laser field as discussed in Sec. III A.

Initial configurations were prepared as follows. To begin with, we performed a MD run in the case where no external field is applied. After the system reached equilibrium, 40 initial configurations were generated at temporally well separated intervals. We defined $t=-10$ ps as the time when each initial configuration was realized. The electric field was applied after $t=0$ ps in each simulation. We performed 40 MD runs for different initial conditions at $t=-10$ ps, and averaged the quantities obtained.

III. RESULTS AND DISCUSSION

A. Simulation results of optical alignment

To determine the spatial orientation of a pyrimidine molecule, χ is defined as the angle between the polarization direction of the electric field (Z) and the principal axis having the largest polarizability in a pyrimidine molecule (y axis in Fig. 1). The values of $\cos\chi=\pm1$ mean completely aligned states.

Two trajectories of $\cos\chi$ in the case of $E_0=1.5\times10^{10}$ V/m (light intensity$=3.0\times10^{13}$ W/cm^2) are shown in Fig. 2. Individual trajectories in 40 MD runs seem different from each other because of the difference in the initial conditions, some trajectories showing complete alignment and some not. In Fig. 2(a), a tendency toward alignment is observed after $t=0$ ps. The value of $\cos\chi$ indicates 0.8–1.0 after $t=15$ ps; the alignment is nearly complete. In contrast, Fig. 2(b) shows that the value of $\cos\chi$ fluctuates between −0.5 and 0.4 after $t=0$ ps; there is little tendency toward alignment. Large leaps in $\cos\chi$ observed in Figs. 2(a) and 2(b) indicate that water molecules collide with the pyrimidine molecule with large momenta. The stochastically generated large torque on the pyrimidine molecule can change the fate of alignment dynamics.

Because the ensemble average of $\cos\chi$ for different initial conditions is zero, the degree of alignment for a molecule should be quantified by the expectation value of $\cos^2\chi$, $\langle\cos^2\chi\rangle$. An isotropic distribution of the molecular axis shows $\langle\cos^2\chi\rangle=1/3$, whereas a perfectly alignment gives $\langle\cos^2\chi\rangle=1$. The ensemble averages of 40 MD runs are shown in Fig. 3. The solid and dotted lines represent the results of the zeroth-order approximation method and of the first-order approximation method, respectively. Since the applied electric field is absent before $t=0$ ps in these simulations, the state of pyrimidine before $t=0$ ps is isotropic. Figure 3 shows $\langle\cos^2\chi\rangle\simeq1/3$ before $t=0$ ps. Unlike the trajectories of individual MD runs (Fig. 2), the *average* trajectory of 40 MD runs shows a clear tendency toward align-

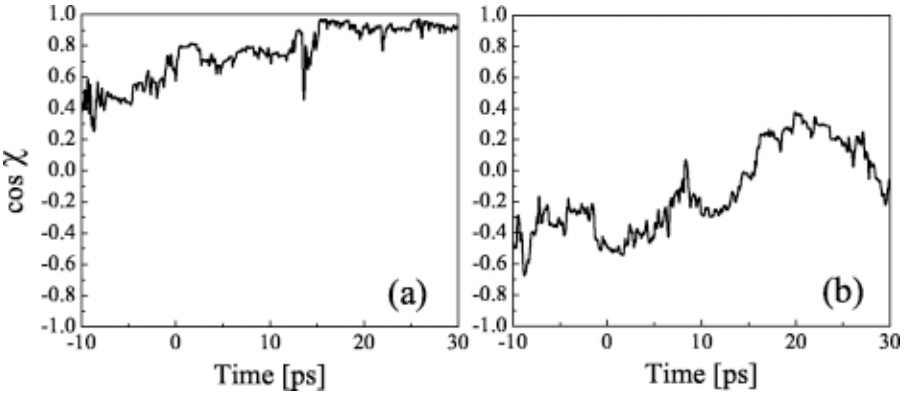

FIG. 2. Two typical trajectories of $\cos\chi$ selected from 40 MD runs for a dilute aqueous solution of pyrimidine. Here, χ is the angle between the field polarization direction Z and the molecular axis of pyrimidine having the largest polarizability. The strength of the applied laser electric field is $E_0=1.5\times10^{10}$ V/m in both cases. The electric field for alignment is turned on at $t=0$ ps. Panel (a) shows that a pyrimidine molecule was forced to be aligned. However, (b) shows little tendency toward alignment. The value of $\cos\chi$ occasionally jumps within a period that is shorter than 1 ps.

ment. On the other hand, water molecules were not aligned in the range of light intensity under consideration.

The first-order approximation method of Eq. (12) contains the interactions between field-induced dipoles, in addition to the zeroth-order term of Eq. (11). However, Fig. 3 only shows a little difference between the zeroth-order and first-order approximation methods. This suggests that the zeroth-order and first-order approximation methods do not give a substantial difference to the results of MD simulations in the presence of an intense laser field.

To justify the truncation in Eq. (7), we estimated the electric field on a molecule due to the field-induced dipoles of the surrounding molecules, $\mathbf{E}_{\mathrm{sur}}=\Sigma_{j\neq i}\mathbf{T}_{ij}\boldsymbol{\alpha}_j$. In a region of the field strength of our simulations ($E_0\sim10^{10}$ V/m), the ratio $\mathbf{E}_{\mathrm{sur}}/\mathbf{E}_{\mathrm{ext}}(t)$ was not more than 10%. In the case where the field-induced dipoles of molecules are not large enough to align molecules, the molecules are almost randomly oriented around a molecule: $\mathbf{E}_{\mathrm{sur}}$ is much weaker than $\mathbf{E}_{\mathrm{ext}}(t)$. In the case of perfect alignment, the field-induced dipoles are parallel to one another: $\mathbf{E}_{\mathrm{sur}}$ is again relatively weak. The relation of $\mathbf{E}_{\mathrm{sur}}\ll\mathbf{E}_{\mathrm{ext}}(t)$ is consistent with the findings that the zeroth-order and first-order approximations do not give any significant differences as shown in Fig. 3. Since $\mathbf{E}_{\mathrm{sur}}\ll\mathbf{E}_{\mathrm{ext}}(t)$, we also presume that the first-order correction term and the effect of higher-order DID interactions are relatively small even if the spherical cutoff for the interaction between the field-induced dipoles is removed by using the Ewald summation technique.[62]

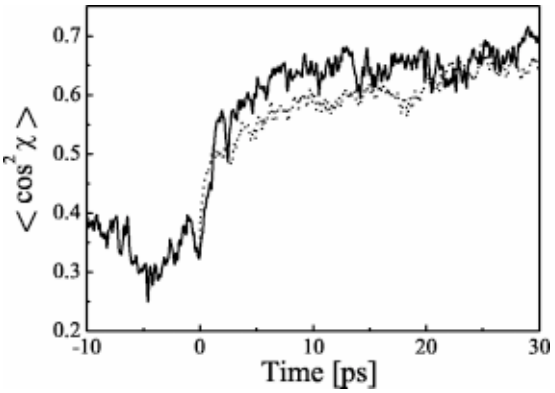

FIG. 3. Ensemble averages $\langle\cos^2\chi\rangle$ of pyrimidine in water. The solid and dotted lines represent the results of the zeroth-order approximation method of Eq. (11) and those of the first-order approximation method of Eq. (12), respectively. $E_0=1.5\times10^{10}$ V/m in both MD simulations.

B. Analysis based on the Fokker–Planck equation

In this section we present the results of theoretical analysis based on stochastic equations. Figure 2 shows an important feature. The value of $\cos\chi$ of a pyrimidine molecule fluctuates rapidly and frequently both in Figs. 2(a) and 2(b), indicating that water molecules collide frequently with the pyrimidine molecule. The collisions allow us to neglect inertial effects of the pyrimidine molecule. For this reason, we can describe the rotational motion of the pyrimidine molecule as a Brownian motion under a potential. In this condition, for a linear molecule, we obtain a Langevin equation,

$$I\frac{d\omega}{dt}=-\frac{\partial U_{\mathrm{pol}}^{\mathrm{lincar}}}{\partial\theta}-I\gamma\omega+\xi(t), \tag{24}$$

where I is the moment of inertia, $U_{\mathrm{pol}}^{\mathrm{linear}}$ is the polarization energy defined in Eq. (22); ω is the angular velocity, γ is the friction constant, and $\xi(t)$ is the noise representing all of the stochastic effects.

If $\xi(t)$ is Gaussian white noise, $\xi(t)$ has the following properties:

$$\langle\xi(t)\rangle=0, \tag{25}$$

$$\langle\xi(t)\xi(t')\rangle=2k_BT\gamma I\delta(t-t'), \tag{26}$$

where $\langle\cdot\rangle$ expresses the time average, T is the temperature (298 K), k_B is the Boltzmann constant, and $\delta(t)$ is the Dirac delta function. In the case of Gaussian white noise, a Fokker–Planck equation is derived from the Langevin equation. Additionally, we can expand this discussion to three-dimensional (3D) cases in which the polarization energy is expressed by Eq. (21). The 3D Fokker–Planck equation for the orientational probability, $f(\phi,\theta,\psi,t)$, in the Euler angle representation is known to be given by[63,64]

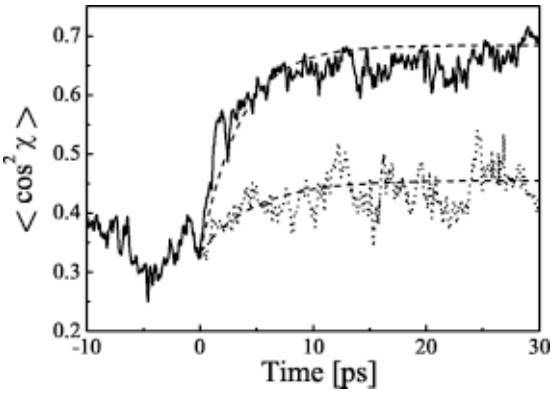

FIG. 4. Degree of alignment, $\langle \cos^2 \chi \rangle$, in MD simulations and theoretical analyses based on the Fokker–Planck equation. The solid and dotted lines represent the results of MD simulations at $E_0 = 1.5 \times 10^{10}$ V/m and 0.8×10^{10} V/m, respectively. The smooth dashed lines are the corresponding solutions of the Fokker–Planck equation. The rotational diffusion coefficient used is $D_x = 2.75 \times 10^{10}$ s^{-1}.

$$\frac{\partial f}{\partial t} = D_x \left\{ \frac{\cos\theta}{\sin\theta} \frac{\partial f}{\partial \theta} + \frac{\cos^2\theta}{\sin^2\theta} \frac{\partial^2 f}{\partial^2 \psi} + \frac{\partial^2 f}{\partial^2 \theta} \right\} + 2D_x \frac{\partial^2 f}{\partial^2 \psi} + 2D_x \frac{\partial}{\partial \psi} \left(f \frac{1}{k_B T} \frac{\partial U^o_{\mathrm{pol}}}{\partial \psi} \right) + D_x \left\{ \frac{\cos\theta}{\sin\theta} f \frac{1}{k_B T} \frac{\partial U^o_{\mathrm{pol}}}{\partial \theta} + \frac{\cos^2\theta}{\sin^2\theta} \frac{\partial}{\partial \psi} \left(f \frac{1}{k_B T} \frac{\partial U^o_{\mathrm{pol}}}{\partial \psi} \right) + \frac{\partial}{\partial \theta} \left(f \frac{1}{k_B T} \frac{\partial U^o_{\mathrm{pol}}}{\partial \theta} \right) \right\}, \tag{27}$$

where the inertial effects are neglected (the Smoluchowski limit), and D_i is the rotational diffusion coefficients (where $i = x$, y, and z):

$$D_i = \frac{k_B T}{\gamma I_i}. \tag{28}$$

We assumed that the relation $D_x = D_y = 1/2 D_z$ approximately holds because of the shape of a pyrimidine molecule.

We solved Eq. (27) for the condition of initial probability density being isotropic. The solution of Eq. (27) gives the time-dependent value for the degree of alignment. Figure 4 shows $\langle \cos^2 \chi \rangle$ of MD simulations using the zeroth-order approximation method at two different field intensities and the corresponding results obtained from the Fokker–Planck equation. The rotational diffusion coefficients used in Eq. (27) were determined so that the average of $\cos^2 \chi$ obtained from the Fokker–Planck equation adequately reproduced the results of MD simulations, as shown below.

Figure 5 shows the degrees of deviation between MD results and the corresponding results obtained by using the Fokker–Planck equation as a function of the rotational diffusion coefficient D_x. The degree of deviation, σ, is defined as

$$\sigma = \sqrt{\frac{1}{N} \sum_i^N \{ \langle \cos^2 \chi^{\mathrm{MD}}(t_i) \rangle - \langle \cos^2 \chi^{\mathrm{FP}}(t_i) \rangle \}}, \tag{29}$$

where N is the number of data points in a time domain ($t_i = 0-30$ ps in Fig. 4), $\langle \cos^2 \chi^{\mathrm{MD}}(t_i) \rangle$ is the average value for MD simulations, and $\langle \cos^2 \chi^{\mathrm{FP}}(t_i) \rangle$ is the value for the Fokker–Planck equation. The minima in Figs. 5(a) and 5(b) for different light intensities agree well with each other. The order of the rotational diffusion coefficients determined from the locations of the minima ($\sim 10^{10}$ s^{-1}) is reasonable as molecular rotational diffusion coefficients.[65] This indicates that the temporal scale of molecular alignment in our MD simulations is valid.

Here we comment on the intensity of the laser fields used in the simulations. The analysis in this subsection allows us to consider molecular alignment in a liquid phase by using the simple model described by the Fokker–Planck equation. The solution of the Fokker–Planck equation (27) at the steady state limit gives the probability density in compliance with a Boltzmann distribution. We can write an expectation value of the degree of alignment $\langle \cos^2 \chi \rangle$ in a steady state as

$$\langle \cos^2 \chi \rangle = \frac{\int_0^{\pi} d\theta \int_0^{2\pi} d\psi (\sin\theta \sin\psi)^2 \sin\theta \exp\{-U^o_{\mathrm{pol}}/(k_B T)\}}{+\int_0^{\pi} d\theta \int_0^{2\pi} d\psi \sin\theta \exp\{-U^o_{\mathrm{pol}}/(k_B T)\}}. \tag{30}$$

As indicated in Fig. 4, the steady state value of $\langle \cos^2 \chi \rangle$ calculated from Eq. (30) is 0.684 at $E_0 = 1.5 \times 10^{10}$ V/m and it is 0.455 at $E_0 = 0.8 \times 10^{10}$ V/m. This equation could be

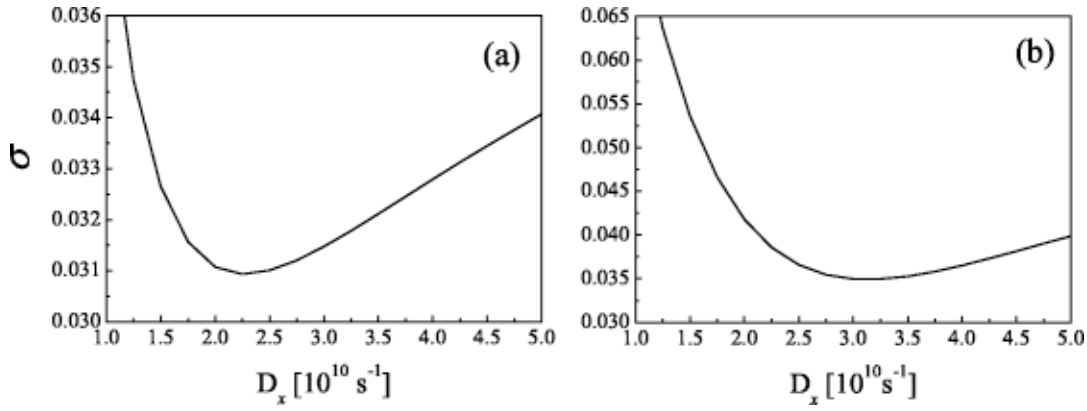

FIG. 5. Degrees of deviations between the results of MD simulations and those of Fokker-Planck theoretical analyses as a function of the rotational diffusion coefficient D_x: (a) Strength of the applied laser electric field $E_0 = 0.8 \times 10^{10}$ V/m; (b) $E_0 = 1.5 \times 10^{10}$ V/m.

used for estimating the degree of alignment simply. It is known that molecules are rapidly ionized at intensity $I \gtrsim 10^{14}$ W/cm^2 ($E_0 \gtrsim 2.7\times 10^{10}$ V/m). However, we predict from Eq. (30) that alignment effects would emerge at lower laser intensity of $I\sim 10^{12}$ W/cm^2 in a liquid phase of molecules having anisotropic polarizabilities over 100 Å^3.

C. Differences between the mechanisms of optical alignment in a liquid phase and a gas phase

We begin with explaining the mechanism of optical alignment in a gas phase.[8,14] A molecule in a nonresonant optical field experiences an effective anisotropic potential of which the minimum exists in the polarization direction of the field. The eigenstates for quantized molecular rotation in the presence of an electric field are called pendular states. The wave function of a low pendular state is localized near the potential minimum. If the electric field is turned on adiabatically, i.e., in a time scale much longer than the rotational period $2\pi/B$, a field-free rotational state, $|\tilde{J}M\rangle$, is correlated with a pendular state labeled by the quantum numbers $\tilde{J}$ and M. As the field intensity increases gradually in a pulse, the rotational state changes adiabatically from a field-free isotropic state to an anisotropic pendular state: by using a pulse that has a duration longer than the rotational period, it is possible to adiabatically align molecules in a gas phase. For instance, an iodine molecule, I_2, has a rotational period $2\pi/B\sim 1$ ns (where $B=0.037$ cm^{-1}). Thus, I_2 is aligned by *nanosecond* YAG laser pulses of $I\sim 10^{12}$ W/cm^2. In this range of intensities, ionization hardly occurs.

As in a gas phase, a laser field creates an effective anisotropic potential for alignment in a liquid phase. However, in a liquid phase, collisions between molecules occur more or less continuously. Unlike in a gas phase, stochastic rotational torque is also generated by collisions with solvent molecules. Therefore, the time scale needed for alignment in a liquid phase is different from that in a gas phase. In the case of adiabatic alignment in a gas phase, the time scale required is longer than the rotational period.[8,14] On the other hand, in a liquid phase, the rotational diffusion under the anisotropic potential causes alignment. The time required for alignment is thus in the order of the time scale of rotational diffusion, i.e., the reciprocals of rotational diffusion coefficients. For instance, the time required for alignment of a pyrimidine molecule is over 300 ps in a gas phase, whereas it is about only ~10 ps in a liquid phase as shown in Fig. 4.

IV. CONCLUSIONS

In this paper, we performed MD simulations of field-induced molecular alignment in a dilute aqueous solution of pyrimidine. We formulated in a systematic way the effective forces induced by a nonresonant laser field on the basis of the concept of ''optical cycle average.'' According to the results of the MD simulations, a pyrimidine molecule is aligned in a field of $I\sim 10^{13}$ W/cm^2 and $\lambda = 800$ nm. Analysis of the results of simulations led to the conclusion that temporal behavior of field-induced alignment in a liquid phase is adequately reproduced by the solution of the Fokker–Planck equation for a rotational model system in which environmental fluctuations are represented by Gaussian white noise. The results of this analysis revealed that the time required for alignment in a liquid phase is in the order of the reciprocals of rotational diffusion coefficients. The time scale for alignment is thus nearly independent of field intensity. In addition, it was confirmed that the degree of alignment at the steady state limit is determined by a Boltzmann distribution. Thus, the anisotropy of the polarizability of a molecule, light intensity, and temperature determine the degree of alignment at the steady state limit, as shown in Eq. (30). While the steady state value of the alignment of a solute molecule is independent of the solvent, the time required for reaching the steady state depends on the solvent.

In this study, we focused on the interaction of an aqueous solution with a nonresonant laser field. To discuss microscopic dynamics of molecules in a liquid interacting with electronically resonant fields, excitation processes and subsequent dynamical processes such as *cis–trans* isomerization must be included in the MD simulation. The dynamical features of this kind of isomerization in a viscous matrix such as a polymer should be investigated in a future study.

ACKNOWLEDGMENTS

We thank Professor Motohiko Tanaka, Dr. Toshiaki Iitaka, and Dr. Koji Hatanaka for their valuable discussions. This work was supported in part by a grant-in-aid for scientific research (No. 14540463) and a grant-in-aid for scientific research on priority areas, ''Control of Molecules in Intense Laser Field'' (Area No. 419) from the Ministry of Education, Culture, Sports, Science and Technology, Japan.

[1] C. S. Adams and E. Riis, Prog. Quantum Electron. **21**, 1 (1997).
[2] Y. Sato, H. Kono, S. Koseki, and Y. Fujimura, J. Am. Chem. Soc. **125**, 8019 (2003).
[3] A. Hishikawa, A. Iwamae, and K. Yamanouchi, Phys. Rev. Lett. **83**, 1127 (1999).
[4] A. Assion, T. Baumert, M. Bergt, T. Brixner, B. Kiefer, V. Seyfried, M. Strehle, and G. Gerber, Science **282**, 919 (1998).
[5] J. R. Levis, G. M. Menkir, and H. Rabitz, Science **292**, 709 (2001).
[6] B. Friedrich and D. Herschbach, Nature (London) **353**, 412 (1991).
[7] H. J. Loesch, Annu. Rev. Phys. Chem. **46**, 555 (1995).
[8] B. Friedrich and D. Herschbach, Phys. Rev. Lett. **74**, 4623 (1995).
[9] J. D. Weinstein, R. deCarvalho, T. Guillet, B. Friedrich, and J. M. Doyle, Nature (London) **395**, 148 (1998).
[10] T. Takekoshi, B. M. Patterson, and R. J. Knize, Phys. Rev. Lett. **81**, 5105 (1998).
[11] H. Stapelfeldt, H. Sakai, E. Constant, and P. B. Corkum, Phys. Rev. Lett. **79**, 2787 (1997).
[12] W. Kim and P. M. Felker, J. Chem. Phys. **104**, 1147 (1996).
[13] W. Kim and P. M. Felker, J. Chem. Phys. **108**, 6763 (1998).
[14] J. J. Larsen, H. Sakai, C. P. Safvan, I. Wendt-Larsen, and H. Stapelfeldt, J. Chem. Phys. **111**, 7774 (1999).
[15] H. Stapelfeldt and T. Seideman, Rev. Mod. Phys. **75**, 543 (2003).
[16] J. J. Larsen, K. Hald, N. Bjerre, H. Stapelfeldt, and T. Seideman, Phys. Rev. Lett. **85**, 2470 (2000).
[17] D. M. Villeneuve, S. A. Aseyev, P. Dietrich, M. Spanner, M. Y. Ivanov, and P. B. Corkum, Phys. Rev. Lett. **85**, 542 (2000).
[18] F. Weigert, Z. Phys. **5**, 410 (1921).
[19] N. S. Neporent and O. V. Stolbova, Opt. Spectrosc. **14**, 331 (1963).
[20] M. Dumont, Z. Sekkat, R. Loucif-Saibi, K. Nakatani, and J. A. Delaire, Mol. Cryst. Liq. Cryst. Sci. Technol., Sect. B: Nonlinear Opt. **5**, 395 (1993).
[21] J. A. Delaire and K. Nakatani, Chem. Rev. **100**, 1817 (2000).
[22] F. Charra, F. Devaux, J.-M. Nunzi, and P. Raimond, Phys. Rev. Lett. **68**, 2440 (1992).

[23] J.-M. Nunzi, F. Charra, C. Fiorini, and J. Zyss, Chem. Phys. Lett. **219**, 349 (1994).
[24] M. Dumont, Mol. Cryst. Liq. Cryst. A **282**, 437 (1996).
[25] T. Brixner and G. Gerber, Phys. Chem. Chem. Phys. **4**, 418 (2003).
[26] M. W. Evans, J. Chem. Phys. **76**, 5473 (1982).
[27] M. W. Evans, J. Chem. Phys. **76**, 5480 (1982).
[28] M. W. Evans, J. Chem. Phys. **77**, 4632 (1982).
[29] M. W. Evans, J. Chem. Phys. **78**, 5403 (1983).
[30] Y. W. Tang, I. Szalai, and K.-Y. Chan, Mol. Phys. **100**, 1497 (2002).
[31] J. Petravic and J. Delhommelle, J. Chem. Phys. **119**, 8511 (2003).
[32] P. Ahlström, A. Wallqvist, S. Engström, and B. Jönsson, Mol. Phys. **68**, 563 (1989).
[33] D. N. Bernardo, Y. Ding, K. K. Jespersen, and R. M. Levy, J. Phys. Chem. **98**, 4180 (1994).
[34] T. M. Nymand and P. Linse, J. Chem. Phys. **112**, 6152 (2000).
[35] K. Miller, J. Am. Chem. Soc. **112**, 8543 (1990).
[36] P. T. V. Duijnen and M. Swart, J. Phys. Chem. A **102**, 2399 (1998).
[37] B. T. Thole, Chem. Phys. **59**, 341 (1981).
[38] M. Sprik and M. L. Kline, J. Chem. Phys. **89**, 7556 (1988).
[39] S.-B. Zhu, S. Yao, J.-B. Zhu, S. Singh, and G. W. Robinson, J. Phys. Chem. **95**, 6211 (1991).
[40] S.-B. Zhu, J.-B. Zhu, and G. W. Robinson, Phys. Rev. A **44**, 2602 (1991).
[41] S. W. Rick, S. J. Stuart, and B. J. Berne, J. Chem. Phys. **101**, 6141 (1994).
[42] H. A. Stern, F. Rittner, B. J. Berne, and R. A. Friesner, J. Chem. Phys. **115**, 2237 (2001).
[43] N. J. English and J. M. D. MacElroy, J. Chem. Phys. **119**, 11806 (2003).
[44] J. L. Banks, G. A. Kaminski, R. Zhou, D. T. Mainz, B. J. Berne, and R. A. Friesner, J. Chem. Phys. **110**, 741 (1999).
[45] D. Frenkel and J. P. McTague, J. Chem. Phys. **72**, 2801 (1980).
[46] B. M. Ladanyi, J. Chem. Phys. **78**, 2189 (1983).
[47] B. M. Ladanyi and Y. Q. Liang, J. Chem. Phys. **103**, 6325 (1995).
[48] S. Califano, V. Schettino, and N. Neto, *Lattice Dynamics of Molecular Crystals* (Springer, Berlin, 1981), Chap. 3.
[49] L. C. Geiger and B. M. Ladanyi, J. Chem. Phys. **87**, 191 (1987).
[50] L. C. Geiger and B. M. Ladanyi, J. Chem. Phys. **89**, 6588 (1988).
[51] L. C. Geiger, B. M. Ladanyi, and M. E. Chapin, J. Chem. Phys. **93**, 4533 (1990).
[52] M. Paolantoni and B. M. Ladanyi, J. Chem. Phys. **117**, 3856 (2002).
[53] M. P. Allen and D. J. Tildesley, *Computer Simulation of Liquids* (Clarendon, Oxford, 1987).
[54] H. Kono and S. Koseki, in *Laser Control and Manipulation of Molecules*, edited by A. D. Bandrauk, R. J. Gordon, and Y. Fujimura (Oxford University Press, Oxford, 2002), Chap. 18, p. 267.
[55] Euler angles are defined as follows. Beginning with a body-fixed axis system x,y,z and a space-fixed axis system X,Y,Z, in coincidence, the body-fixed system is moved to its final orientation in three steps. First, the body is rotated by an angle ϕ about the z axis. We call the new position of the body-fixed axis system x', y', z'. The second step is rotation of the body about the x' axis by an angle θ. The new position of the body-fixed axis system is called x'', y'', z''. Finally, the body is rotated about z'' axis by an angle ψ. Then the final position x''', y''', z''' is obtained.
[56] J. Zeng, J. S. Craw, N. S. Hush, and J. R. Reimers, J. Chem. Phys. **99**, 1482 (1993).
[57] W. L. Jorgensen, J. Chandrasekhar, J. D. Madura, R. W. Impey, and M. L. Klein, J. Chem. Phys. **179**, 926 (1983).
[58] M. W. Mahoney and W. L. Jorgensen, J. Chem. Phys. **112**, 8910 (2000).
[59] C. Huiszoon, Mol. Phys. **58**, 865 (1986).
[60] B. Shanker and J. Applequist, J. Phys. Chem. **100**, 3887 (1996).
[61] D. J. Evans and G. P. Morriss, *Statistical Mechanics of Nonequilibrium Liquids* (Academic, London, 1990).
[62] Z. Wang and C. Holm, J. Chem. Phys. **115**, 6351 (2001).
[63] R. M. Mazo, *Brownian Motion: Fluctuations, Dynamics, and Applications* (Clarendon, Oxford, 2002).
[64] N. G. V. Kampen, *Stochastic Processes in Physics and Chemistry* (North–Holland, Amsterdam, 1981).
[65] C. J. F. Böttcher and P. Bordewijk, *Theory of Electric Polarization*, 2nd completely rev. ed. (Elsevier, Amsterdam, 1978).